AD-A089 217 WISCONSIN UNIV-MADISON DEPT OF CHEMISTRY F/G 7/4
THERMAL MANIPULATION OF DEACTIVATION PROCESSES IN LUMINESCENT P--ETC(U)
AUG 80 B R KARAS, D J MORANO, D K BILICH N00014-78-C-0633
UNCLASSIFIED TR-4 NL

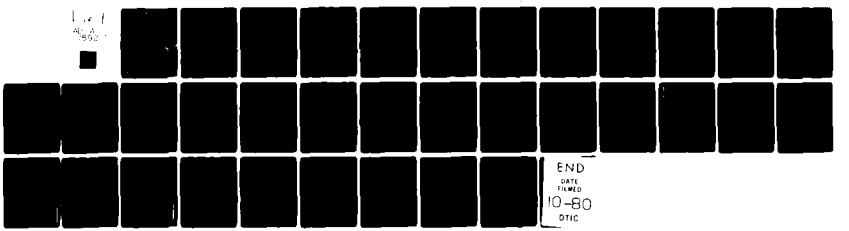

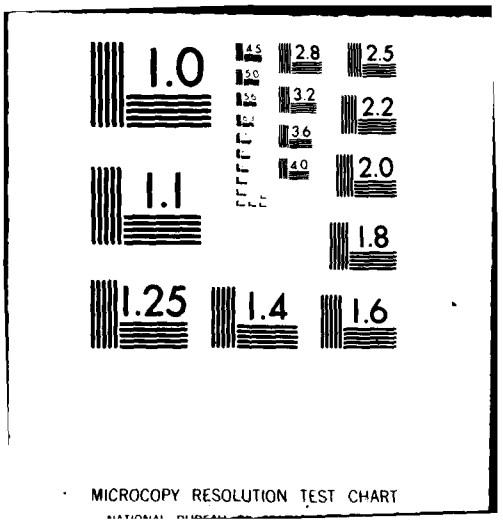
1.0
1.1
1.25
1.4
1.6
1.8
2.0
2.2
2.5
2.8
3.2
3.6
4.0
4.5
5.0
MICROCOPY RESOLUTION TEST CHART

LEVEL II

OFFICE OF NAVAL RESEARCH

Contract No. N00014-78-C-0633

Task No. NR 051-690

TECHNICAL REPORT NO. 4

Thermal Manipulation of Deactivation Processes in Luminescent Photoelectrochemical Cells Employing Tellurium-Doped Cadmium Sulfide Photoelectrodes

by

Bradley R. Karas, David J. Morano, Daniel K. Bilich and Arthur B. Ellis*

Prepared for publication

in the

Journal of the Electrochemical Society

Department of Chemistry
University of Wisconsin
Madison, Wisconsin 53706

August 12, 1980

*To whom all correspondence should be addressed.

380155

Unclassified

SECURITY CLASSIFICATION OF THIS PAGE (When Data Entered)

REPORT DOCUMENTATION PAGE		READ INSTRUCTIONS BEFORE COMPLETING FORM
1. REPORT NUMBER Technical Report No. 4	2. GOVT ACCESSION NO. ADA089 217	3. RECIPIENT'S CATALOG NUMBER
4. TITLE (and Subtitle) Thermal Manipulation of Deactivation Processes in Luminescent Photoelectrochemical Cells Employing Tellurium-Doped Cadmium Sulfide Photoelectrodes		5. TYPE OF REPORT & PERIOD COVERED 6. PERFORMING ORG. REPORT NUMBER
7. AUTHOR(s) Bradley R. Karas, David J. Morano, Daniel K. Bilich, and Arthur B. Ellis		8. CONTRACT OR GRANT NUMBER(s) N00014-78-C-0633
9. PERFORMING ORGANIZATION NAME AND ADDRESS Department of Chemistry, University of Wisconsin Madison, Wisconsin 53706		10. PROGRAM ELEMENT, PROJECT, TASK AREA & WORK UNIT NUMBERS NR 051-690
11. CONTROLLING OFFICE NAME AND ADDRESS Office of Naval Research/Chemistry Program Arlington, Virginia 22217		12. REPORT DATE August 12, 1980 13. NUMBER OF PAGES 27
14. MONITORING AGENCY NAME & ADDRESS(if different from Controlling Office)		15. SECURITY CLASS. (of this report) Unclassified 15a. DECLASSIFICATION/DOWNGRADING SCHEDULE

16. DISTRIBUTION STATEMENT (of this Report)

Approved for Public Release: Distribution Unlimited.

17. DISTRIBUTION STATEMENT (of the abstract entered in Block 20, if different from Report)

18. SUPPLEMENTARY NOTES

Prepared for publication in the Journal of the Electrochemical Society

19. KEY WORDS (Continue on reverse side if necessary and identify by block number)

photoelectrochemistry, luminescence, temperature effects; optical energy conversion

20. ABSTRACT (Continue on reverse side if necessary and identify by block number)

Temperature significantly modifies the efficiencies of luminescence and photocurrent in an n-type, single crystal, CdS:Te-based photoelectrochemical cell (PEC) employing aqueous polyselenide electrolyte. Between 20° and 100°C photocurrent (quantum yield ϕ_x) from ultraband gap 501.7 nm excitation increases modestly by ≤20%, whereas photocurrent from bandgap edge 514.5 nm excitation increases by about an order of magnitude, reaching

DD FORM 1 JAN 73 1473 EDITION OF 1 NOV 65 IS OBSOLETE S/N 0102-LF-014-6601

Unclassified

SECURITY CLASSIFICATION OF THIS PAGE (When Data Entered)

LESS THAN OR =

20. Abstract (continued)

50-100% of the 20°C 501.7 nm photocurrent. Undoped CdS exhibits a similar photocurrent-temperature profile. Higher temperatures thus extend the wavelength response of CdS- and CdS:Te-based PEC's. In contrast to the increase in photocurrent, emissive efficiency (quantum yield ϕ_r) of CdS:Te drops by a factor of ~10-20 over the same temperature range; this decline is relatively insensitive to potential and excitation wavelength (501.7 or 514.5 nm). Little change in the spectral distribution of emission (λ_{max} ~600 nm) is observed with temperature. A dependence of emission intensity on potential is observed for the first time with 514.5 nm excitation in the high temperature regime. These results are interpreted in terms of band bending, optical penetration depth, the known red-shift of the CdS bandgap edge with temperature, and the competitive nature of emission and photocurrent. Relationships among ϕ_x, ϕ_r, and ϕ_{r_o}/ϕ_r (out-of-circuit to in-circuit emission intensity) are discussed.

This article has been published: J. Electrochem. Soc. 127, 1144 (1980).

Introduction

We recently reported that n-type tellurium-doped CdS (CdS:Te) serves as a luminescent photoelectrode in photoelectrochemical cells (PECs) used to convert optical energy to electricity.[1] In this manner CdS:Te permits determination of the effect of PEC parameters such as incident excitation wavelength, electrolyte, and potential upon the various deactivation routes of the semiconductor electrode excited state. In particular, luminescence is a probe of electron-hole recombination processes which compete with electron-hole separation leading to photocurrent.

In the course of our studies, we noted that the emission intensity and, in some instances, the photocurrent of CdS:Te-based PECs were temperature dependent. We demonstrate herein that temperature may be used to significantly modify the relative efficiencies of excited state deactivation pathways in a manner which underscores the competitive nature of luminescence and photocurrent. In addition, higher temperatures extend the wavelength response of both CdS- and CdS:Te-based PECs.

Theory

The band gap of undoped CdS, E_{BG}, is ~2.4 eV at 298°K.[2] Although CdS:Te has a low energy tail in its absorption spectrum which masks the band gap, the highest absorptivities ($>10^4$ cm^{-1}) occur at $\lambda \lesssim 500$ nm in both undoped CdS and CdS:Te.[2-6] Ultraband gap wavelengths are therefore taken as those with $\lambda \lesssim 500$ nm; absorption occurs within ~0.1-1 μ of the surface, a distance typically corresponding to the depletion region. This zone is characterized by maximum band bending and is conducive to ready separation of photogenerated electron-hole (e^--h^+) pairs leading to maximum photocurrent.[7]

Longer excitation wavelengths penetrate farther into the crystal and the diminished band bending favors e^--h^+ recombination at the expense of separation. Luminescent CdS:Te-based PECs exhibit more emission and less photocurrent with band gap edge 514.5 nm than with ultraband gap 501.7 nm excitation, for example.[1]

Figure 1a illustrates the interrelationship of penetration depth and band bending at these wavelengths. The dashed line represents the discrete states involved in the emissive process which are introduced by the Te dopant; holes trapped at Te sites (Te presumably substitutes for S in the lattice) may coulombically bind an electron in or near the conduction band to form an exciton whose subsequent radiative collapse leads to luminescence.[3-6]

Our chief guide for predicting thermal effects in the PEC was the known optical band gap temperature coefficient, dE_{BG}/dT, for undoped CdS. This coefficient has a value of -5.2×10^{-4} eV/°K between 90° and 400°K.[8] To the extent that CdS:Te resembles CdS, this relationship predicts that the band gap edge red shifts with increasing temperature; at a sufficiently high temperature 514.5 nm will become an ultraband gap wavelength like 501.7 nm, for example. Figures 1b and c illustrate the anticipated effect of increased temperature on the band diagram and absorption spectrum. The decline of E_{BG} with increasing temperature has been interpreted as arising from two effects: lattice dilation and energy level broadening at the edges of the band gap due to collisions between electrons and phonons.[9]

Implicit in the comparison of Figures 1a and b is the relative insensitivity of the depletion region width, W, to temperature. The expression for W is given by equation (1) where

$$W = (2\varepsilon\varepsilon_o V_B/qN)^{1/2} \qquad (1)$$

N is the charge carrier density in the semiconductor, q is the electronic charge, ε_o is the permittivity of free space, ε is the semiconductor dielectric constant and V_B is the amount of band bending in the depletion region.[10] For a given

electrolyte we do not expect W to change drastically over the 20-100°C temperature range investigated. That is, we are assuming variations in ϵ, N, and V_B to be small. We note that ϵ changes by less than 15% between -196°and 25°C for undoped CdS[11] and that donors in 50 ppm CdS:Te are $\gtrsim$90% ionized at room temperature (Hall measurements).[5] The maximum value of V_B is controlled by the relative energies of the semiconductor Fermi level and the electrolyte redox potential E_{redox}.[7,10] While the explicit temperature dependence of V_B is not known for the electrolyte employed, our results are consistent with small changes in V_B and W. We emphasize that these are assumptions, however, and that a rigorous analysis requires knowledge of the depletion width. With this in mind, we will treat Figure 1 as an approximation whose validity can be qualitatively probed by the PEC of Figure 2.

The PEC consisted of an n-type, single crystal, 100 ppm CdS:Te working electrode, a 2.0 x 0.8 cm Pt foil counterelectrode, a Ag pseudoreference electrode (PRE) and an aqueous polyselenide electrolyte of approximate composition 5M OH^-/0.1M Se^{2-}/0.001M Se_2^{2-}. Temperature control was achieved with resistive heating, as sketched in Figure 2. Emission and photocurrent could be monitored simultaneously by placing the PEC inside an emission spectrometer and inclining the electrode at ~45° with respect to both the Ar ion laser excitation beam and the emission detection optics; the laser beam was expanded and masked to fill the electrode surface. The electrochemistry occurring corresponds to oxidation of polyselenide electrolyte at the photoanode and the reduction of polyselenide at the counter-electrode.[12] No net change occurs in the electrolyte under these conditions, thus permitting sustained conversion of optical energy to electricity while inhibiting the competitive photoanodic dissolution process, equation (2).[12]

$$CdS \xrightarrow{h\nu} Cd^{+2} + S + 2e^- \qquad (2)$$

Polyselenide electrolyte is also an advantageous choice because of its relative transparency to the excitation wavelengths employed.[12]

Results and Discussion

a. Emissive Properties

While $E_{BG} = |E_{CB} - E_{VB}|$ is expected to vary inversely with temperature, the temperature dependence of the CdS:Te emission spectrum will hinge on the relative positions of E_{Te}, E_{CB} and E_{VB}. We and others have found that at 77°K the emission maximum blue-shifts slightly from its 298°K ~600 nm value; the spectrum also sharpens and increases in intensity dramatically.[1,3-6] As the photoelectrode in a PEC, CdS:Te shows little change in the emitted spectral distribution (bandwidth ~5 nm; 550-800 nm) over the ~20°-100°C temperature range investigated in polyselenide electrolyte. A few samples displayed a modest red shift of λ_{max} (~10 nm) and/or more of a low energy tail at the high temperature extreme. Typical spectra obtained at open circuit are shown in Figure 3. In agreement with our earlier studies, the emission spectrum is independent of whether 501.7 or 514.5 nm excitation is used and independent of electrode potential between +0.7 V vs Ag (PRE) and the onset of cathodic current. Changes in potential alter the degree of band bending in an n-type semiconductor: negative bias diminishes and positive bias augments band bending.[7] If the Te state energies were not affected by potential in the same manner as the conduction and valence bands, we would expect to see potential dependent spectral distributions. This not being the case, we show E_{Te} bent in parallel with E_{CB} and E_{VB} in Figures 1a,b.

Another noteworthy feature of Figure 3 is the considerable decline in CdS:Te emission intensity with increasing temperature. The effect is reversible; luminescence reappears with reproducible intensity upon cooling. A more quantitative measure of this effect is provided by Figure 4a which displays the open circuit emission intensity monitored at λ_{max} (600 nm) vs temperature for both excitation wavelengths in polyselenide electrolyte. Earlier studies of CdS:Te in the absence of electrolyte show analogous thermal quenching; plots of $\ell n\ (\frac{I_o}{I_T} - 1)$ vs. T^{-1} (I_o is the maximum emission intensity observed at low temperature; I_T is the emission intensity at temperature T) yielded straight lines over the range of $150° \lesssim T \lesssim 300°K$ and activation energies, corresponding to the exciton binding energy, of ~0.2 eV.[3-5,13] The radiative efficiency is expected to decline from its maximum value, I_o, with increasing temperature, as progressively more thermal energy becomes available to ionize Te-bound holes. We find the rates of decline in emission to be comparable for 514.5 and 501.7 nm excitation. Because emission from the latter is generally weaker,[1b,d] the data in Figure 4a were obtained with 501.7 nm excitation of ~6 times the 514.5 nm intensity in order to match incipient luminescence intensity at room temperature. Note that both curves fall by a factor of ~10-20 over the 75° interval. This factor is comparable to literature data obtained in the absence of electrolyte and with excitation sources consisting of ultraband gap light[3b,5], electron beams [4], and α particles.[13]

We also wished to determine whether the decline in emission intensity with temperature was potential dependent. Figures 4b and c present emission-temperature curves for equivalent numbers of 514.5 and 501.7 nm photons, respectively, at three potentials: open circuit, 0.0 V, and 0.7 V vs Ag (PRE). The irradiated CdS:Te electrode emits more intensely with the longer excitation wavelength so that "100" on Figure 4b represents ~5 times the intensity of "100" on Figure 4c.

To a first approximation the rate of decline in both figures is independent of potential. This is seen more clearly with 514.5 nm excitation where there is very little dependence of emission intensity on potential until high temperatures are reached (vide infra). However, even with the more potential dependent emission intensity from 501.7 nm excitation, the rates of decline are similar as evidenced by the parallel shapes of the three curves. As a unit,Figure 4 indicates that the decline of CdS:Te emission intensity with temperature is relatively insensitive to both penetration depth (501.7 and 514.5 nm) and potential (+0.7 V vs Ag to the onset of cathodic current).

b. iLV curves Simultaneous measurement of current, luminescence, and voltage (iLV curves) as a function of temperature is facilitated by the cell of Figure 2. The emission intensity is conveniently monitored by sitting at a single wavelength, generally λ_{max}. Our previous observations regarding iLV curves for CdS:Te-based PECs at 298°K in aqueous (poly)chalcogenide electrolytes may be summarized as follows: for ultraband gap wavelengths (e.g., 501.7 nm), we observe high quantum efficiencies for electron flow, Φ_x, and potential dependent emissive quantum efficiencies, Φ_r; in general Φ_r and Φ_x vary inversely as a function of potential. For band gap edge (e.g., 514.5 nm) excitation we observe lower values of Φ_x and higher values of Φ_r; however, Φ_r is largely independent of potential.[1]

The ratio of open circuit to in circuit emission intensity, Φ_{r_o}/Φ_r, is a useful expression of the potential dependence with the in circuit value taken at a potential where saturation of photocurrent is evident. For band gap edge excitation Φ_{r_o}/Φ_r is roughly unity, whereas with ultraband gap light we have observed ratios from ~1.2 to as high as 15. To some extent Φ_{r_o}/Φ_r correlates with Φ_x which is invariably low (< 0.1) for band gap edge excitation. Ultraband gap light often gives $0.5 < \Phi_x < 1.0$. By pulsing the electrode between potentials

corresponding to open circuit and maximum photocurrent, the discrepancy of Φ_{r_o}/Φ_r from unity is visibly apparent. The same effect may be observed at different potential sweep rates including point-by-point. We have so frequently observed this phenomenon that we have come to regard it as jointly diagnostic of ultraband gap excitation and a high value of Φ_x.

The prediction afforded by Figure 1 is that increasing the temperature will increase Φ_x for 514.5 nm excitation. Should this occur we would also predict that Φ_{r_o}/Φ_r will exceed unity. In Figure 5a we present plots of photocurrent vs. temperature for 501.7 and 514.5 nm excitation (equal photons/sec) of CdS:Te in aqueous polyselenide electrolyte. The photocurrent at the former wavelength increases by less than 20% over the thermal excursion, but rises by a factor of ~10 with 514.5 nm excitation. In most cases this increase is sufficient to either match the 501.7 nm photocurrent or produce a large fraction ($\gtrsim$ 50%) of it. Since 501.7 nm photocurrent is relatively insensitive to temperature in this range and is not substantially exceeded with shorter wavelength excitation (457.9 nm, e.g.), we regard it as a saturation photocurrent.

Perhaps not surprisingly, undoped CdS yields a similar photocurrent-temperature plot, Figure 5b. Because both undoped CdS and 100 ppm CdS:Te have about the same absorptivity for 514.5 nm light[6], it is difficult to determine what role, if any, the low energy absorption tail of CdS:Te plays in the photocurrent-temperature profile. Longer excitation wavelengths should be helpful in resolving this question. We can say that the rate at which 514.5 nm photocurrent approaches 501.7 nm photocurrent in Figure 5 is in qualitative agreement with the band gap temperature dependence (vide supra). This calculation is made by noting that the two wavelengths differ by ~0.061 eV, predicting a temperature range of ~120° for matching penetration depths from the model and assumptions described above.

Full iLV curves for a CdS:Te-based PEC employing polyselenide electrolyte are presented in Figure 6. Equivalent intensities (photons/sec) of 501.7 and 514.5 nm excitation were used at both room temperature and elevated temperature (49°C for 501.7 nm; 86°C for 514.5 nm). These plots succinctly summarize many of the properties described previously: photocurrent at 23°C is ~18 times greater for 501.7 nm excitation (A vs. B) and emission intensity at open circuit is ~5 times smaller (A' vs. B'). The value of Φ_{r_o}/Φ_r is unity for 514.5 nm (B') and 3.5 for 501.7 nm light (A'). At 49°C photocurrent with 501.7 nm excitation only increased by ~15% (C) but has dramatically increased at 86°C with 514.5 nm light by a factor of almost 8 (D). Emission intensity has dropped by more than a factor of 2 with 501.7 nm light while retaining a similar value of Φ_{r_o}/Φ_r of 3.4 (C'); for the first time and despite its lower absolute intensity, emission from 514.5 nm excitation has resulted in a nonunity value of Φ_{r_o}/Φ_r = 1.27 (D' - note 10-fold scale expansion). We visually confirmed the discrepancy from unity by pulsing the electrode between the extreme voltages shown on curve D'. As mentioned above, this phenomenon is characteristic of larger values of Φ_x. All of the aforementioned changes were reversible simply by returning to the lower temperature.

c. Energy Conversion Efficiency

Another feature of Figure 6 worth noting is the enhancement of optical to electrical energy conversion efficiency at higher temperature with 514.5 nm excitation. The efficiency, η, is given by equation (3). E_V is the output

$$\eta = \frac{\Phi_x E_V}{E_{BG}} \qquad (3)$$

voltage; extraction of this value from i-V curves has been described.[12]

In Table I we present a summary of the energy conversion parameters for both undoped CdS- and CdS:Te-based PECs employing polyselenide electrolyte and a two electrode configuration (photoanode and Pt counterelectrode). The great improvement in η with temperature for 514.5 nm excitation is readily traced to an increase in Φ_x. At higher temperatures η from 514.5 nm excitation begins to rival that obtainable with 501.7 nm light for both electrodes. We do see a decline in output voltage at the higher temperatures; in general the i-V curves shift ~50 - 200 mV anodic between 20° and 100°C. This may indicate, as noted earlier, some difference in the relative energetic positions of the semiconductor Fermi level and E_{redox} with temperature.

While the enhanced red response is certainly desirable from the standpoint of solar energy conversion, we also wished to determine the extent to which it could be sustained. We found that photocurrent from 514.5 nm excitation of CdS:Te at 78±5°C declined at a respectably slow rate of 3%/hr over 9 hrs at a current density of 0.56 mA/cm^2 at 0.08 V vs Ag(PRE). The emission spectrum was unaffected but for its 25% decline in intensity over this period. Neither the optical density of the electrolyte nor its redox potential changed noticeably during the experiment.

d. Implications Regarding Excited State Decay Routes

The striking inverse dependence of photocurrent and emission intensity on temperature depicted in Figures 4-6 highlights their roles as competitive deactivation processes for the CdS:Te electrode excited state. While photocurrent is a unique probe of e^--h^+ pair separation, emission is the minor product of e^--h^+ pair recombination. Nonradiative recombination leading to heat is the dominant recombination process; room temperature emissive efficiencies for 100 ppm CdS:Te are at best only ~1%.[1,3-6]

Our intent has been to probe the manner in which input optical energy is partitioned among the three deactivation paths as a function of PEC parameters.

In steady state experiments such as these, the redistribution of energy is determined using measures of quantum efficiency, Φ_i. Our analysis is necessarily limited because we have only been able to obtain absolute numbers for Φ_x and relative values for Φ_r. We lack measures of Φ_{nr} entirely except insofar as they can be determined by difference, although photothermal spectroscopy has recently been used to provide quantitative information on nonradiative recombination.[14] Despite these limitations, several important features do emerge from the thermal perturbation studies.

First, the ratio of Φ_x to Φ_r can be tuned over many orders of magnitude by a combination of excitation wavelength, electrode potential and temperature. Previous work established the relative insensitivity to potential of Φ_r during excursions where Φ_x was varied from zero (open circuit) to ~0.1 with 514.5 nm excitation.[1] Figures 4-6 demonstrate for 501.7 nm excitation that changes in temperature leave Φ_x relatively constant while Φ_r varies by a factor of up to 20.

Recasting these observations, a given value of Φ_x does not affix unique values to Φ_r and Φ_{nr}. Besides the example just cited, consider Figure 6 in more detail. At room temperature equivalent Φ_x can be achieved with 514.5 nm excitation at +0.7 V or with 501.7 nm excitation at ~-0.62 V vs Ag(PRE). Yet the emission intensity, Φ_r, corresponding to these two conditions is quite different. In a similar vein, a value of Φ_x attained at -0.52 V vs Ag(PRE) with 501.7 nm excitation at room temperature can be matched at 0.7 V with 514.5 nm excitation at 86°C, each condition accompanied by a different Φ_r. These differences can be ascribed to variations in optical penetration depth, band bending, and efficiencies of excited state deactivation processes.

Second, there is now additional evidence linking Φ_x with Φ_{r_o}/Φ_r: (1) ratios exceeding unity for 514.5 nm excitation appear only at elevated temperatures where Φ_x has increased dramatically (Figures 4b and 6); (2) neither Φ_x nor Φ_{r_o}/Φ_r

changed appreciably for 501.7 nm excitation as a function of temperature even though Φ_{r_o} and Φ_r both changed drastically (Figures 4c and 6). A simplistic model correlating Φ_x with Φ_{r_o}/Φ_r can be constructed with the assumption that the ratio of Φ_r to Φ_{nr} is independent of potential (band bending). The ratio Φ_r/Φ_{nr} is, of course, dependent on temperature and optical penetration depth. For the purposes of the model, any recombining e^--h^+ pairs are subject to the Φ_r/Φ_{nr} ratio appropriate for the experimental conditions. Photocurrent serves to divert e^--h^+ pairs from recombining by separating them; at open circuit it plays no role in the excited state description. In passing from a given potential to open circuit, changes in photocurrent are changes in Φ_x and determine how many more e^--h^+ pairs are returned to recombination. The significant quantity is the magnitude of this change relative to how many pairs were recombining before the change, $\Phi_x/(1-\Phi_x)$. This represents the fractional increase expected in Φ_r, equation (4).

$$\frac{\Phi_{r_o}}{\Phi_r} - 1 = \frac{\Phi_x}{1-\Phi_x} \qquad (4)$$

Table II lists typical values of Φ_{r_o}/Φ_r and Φ_x derived from (4). In general, the same logic predicts that Φ_x and Φ_r at any two potentials will be related by (5) for a constant excitation wavelength and temperature.

$$\frac{1-\Phi_{x_2}}{1-\Phi_{x_1}} = \frac{\Phi_{r_2}}{\Phi_{r_1}} \qquad (5)$$

While equations (4) and (5) have been approximately satisfied by several combinations of luminescent electrodes, electrolytes, excitation wavelengths, and temperatures,[1,15,16] they are still oversimplifications. Under certain conditions a nearly mirror image relationship between current and luminescence curves vs. potential has been observed with ZnO photoelectrodes and a derivation presented to account for it.[16] A rigorous model, however, will need to incorporate the following features: (1) nonexponential emission lifetimes[1,3-6]; (2) nonlinear intensity effects on Φ_x and Φ_r[1,6]; (3) local traps, surface imperfections, surface states, grain boundaries, impurity states, etc... all of which can alter Φ_i; (4) electroabsorption (dependence of absorptivity on potential) which mixes optical penetration and band bending effects[17]; (5) conditions leading to humps or plateaus in the luminescence portion of iLV curves - in these regions Φ_r and Φ_x are decidedly not inversely related.[1d] Studies designed to construct a more realistic model are currently in progress.

Experimental

All experiments were performed with ~5x5x1 mm plates of single crystal 100 ppm CdS:Te or undoped CdS obtained from Cleveland Crystals, Cleveland, Ohio. The ~5x5 mm face is oriented perpendicular to the c-axis and sample resistivities are ~2 Ω-cm. Crystals were etched with Br_2/MeOH (1:10 v/v) before use. Electrode and polyselenide electrolyte preparation has been described previously.[1d]

The basic PEC configuration, illustrated in Figure 2, was assembled inside an Aminco-Bowman SPF-2 Spectrophotofluorometer when emission data were desired; the photoelectrode was inclined at ~45° to both the incident Coherent Radiation CR-12 Ar ion laser beam (501.7 or 514.5 nm) and the emission detection optics. The ~3 mm dia beam was 10X expanded and masked to fill the electrode surface. A 0.03M $Na_2Cr_2O_7$ solution was placed in front of the detection optics to filter the exciting light. In experiments where only current-voltage data were obtained, the PEC was simply set on a stir plate and the electrode irradiated "head-on". The electrochemical instrumentation has been described previously.[1d]

Temperatures in the PEC were maintained by resistive heating employing a nichrome wire and a Sepco variable transformer. A thermometer accurate to ± 1°C was calibrated by measuring melting points of several solids; adjustment of its immersion depth into the electrolyte indicated that significant thermal gradients were absent.

Changes in electrolyte absorption over the thermal excursion were probed by single beam experiments using the 501.7 and 514.5 nm laser lines and found to be small (<5% change in %T in a 1 mm pathlength). Light intensity in this and other experiments was measured with a Tektronix J16 radiometer equipped with a J6502 probe head.

The suitability of the 25x0.5 mm dia Ag wire as a PRE was checked by measuring its potential vs. that of a 2.0x0.8 cm Pt foil electrode with a high impedance Data Precision 1450 multimeter. Between 20° and 100°C potential only varied from 100 to 123 mV and was stable for minutes at a time at temperatures in this range. Moreover, i-V curves run at several temperatures with an Ag(PRE) or an SCE were practically superimposable. Energy conversion efficiencies at all temperatures were derived using a two electrode PEC (semiconductor and Pt counterelectrode; reference and counterelectrode leads from the potentiostat wereshorted) whose i-V curves also matched those obtained with an Ag(PRE) or SCE three-electrode PEC. The Pt electrode exhibited good reversibility for the polyselenide redox couple over the entire temperature range.

Curves of photocurrent and emission intensity (monitored at ~600 nm) vs. temperature were obtained by heating from 20-100°C over a span of 80 minutes with readings taken ~every 5°. Reproducibility of the data upon cooling was generally better than ± 10 %. The procedure and equipment involved in the sustained PEC experiment have been described.[1d]

Acknowledgment We thank the Office of Naval Research for their generous support of this work. BRK is grateful to the Electrochemical Society for Summer Support through a Joseph W. Richards Fellowship. Professors John Wiley and Dennis Evans are acknowledged for several helpful discussions.

References

1. (a) A. B. Ellis and B. R. Karas, J. Am. Chem. Soc., 101, 236 (1979); (b) A. B. Ellis and B. R. Karas, Adv. Chem. Ser., in press; (c) A. B. Ellis and B. R. Karas, Abstract #65, 176th ACS Meeting, Miami Beach, Sept. 1978; (d) B. R. Karas and A. B. Ellis, J. Am. Chem. Soc., 102, 0000.
2. D. Dutton, Phys. Rev., 112, 785 (1958).
3. (a) A. C. Aten and J. H. Haanstra, Phys. Lett., 11, 97 (1964); (b) A. C. Aten, J. H. Haanstra, and H. deVries, Philips Res. Rept., 20, 395 (1965).
4. J. D. Cuthbert and D. G. Thomas, J. Appl. Phys., 39, 1573 (1968).
5. D. M. Roessler, ibid., 41, 4589 (1970).
6. P. F. Moulton, Ph.D. Dissertation, Massachusetts Institute of Technology, 1975.
7. H. Gerischer, J. Electroanal. Chem., 58, 263 (1975).
8. R. H. Bube, Phys. Rev., 98, 431 (1954).
9. A. R. Hutson in "Semiconductors", N. B. Hannay, Ed., ACS Monograph Ser. No. 140, Reinhold Publ. Corp., New York, N.Y., 1959, p. 578-80.
10. A. J. Nozik, Ann. Rev. Phys. Chem., 29, 189 (1978).
11. D. Berlincourt, H. Jaffe, and L. R. Shiozawa, Phys. Rev., 129, 1009 (1963).
12. A. B. Ellis, S. W. Kaiser, J. M. Bolts, and M. S. Wrighton, J. Am. Chem. Soc., 99, 2839 (1977).
13. J. E. Bateman, F. E. Ozsan, J. Woods, and J. R. Cutter, J. Phys. D. App. Phys., 7, 1316 (1974).
14. A. Fujishima, G. H. Brilmeyer, and A. J. Bard in "Semiconductor Liquid-Junction Solar Cells", A. Heller, Ed., Proc. Vol. 77-3, Electrochemical Society, Inc., Princeton, N.J., 1977, p. 172.
15. K. H. Beckmann and R. Memming, This Journal, 116, 368 (1969).
16. G. Petermann, H. Tributsch, and R. Bogomolni, J. Phys. Chem., 57, 1026 (1972).
17. D. F. Blossey and P. Handler in "Semiconductors and Semimetals," Vol. 9, R. K. Willardson and A. C. Beer, Eds., Academic Press, New York, N.Y., 1972, p. 302-4.

Table I. Optical to Electrical Energy Conversion Parameters [a]

Electrode	T,°C	$\lambda_{exc.}$	η_{max} [b]	E_V,V [c]	$\Phi_x @ \eta_{max}$ [d]	$\Phi_{x\ max}$ [e]
CdS:Te	23	501.7	5.6	0.32	0.44	0.75
		514.5	0.27	0.28	0.02	0.04
	73	501.7	3.8	0.21	0.44	0.74
		514.5	1.0	0.18	0.14	0.26
CdS	24	501.7	5.0	0.27	0.46	0.68
		514.5	0.21	0.27	0.02	0.03
	73	501.7	2.5	0.19	0.32	0.68
		514.5	0.92	0.24	0.09	0.20

[a] The indicated crystal served as the photoanode in a PEC similar to that shown in Figure 2, but with only two electrodes (Pt counterelectrode and photoanode). Electrolyte composition is 5M OH^-/0.3M Se^{2-}/0.001M Se_2^{2-}. Table entries represent typical values.

[b] Maximum efficiency for optical to electrical energy conversion as defined by equation (3).

[c] Output voltage at η_{max}.

[d] Quantum efficiency for e^- flow at η_{max} ($\pm$ 15%), uncorrected for reflection losses and electrolyte absorption.

[e] Maximum quantum efficiency ($\pm$ 15%) for e^- flow, measured at ~0.7 V vs. Ag(PRE), uncorrected for reflection losses and electrolyte absorption.

Table II. Relationship Between Φ_x and Φ_{r_o}/Φ_r [a]

Φ_x	Φ_{r_o}/Φ_r
0.001	1.00
0.01	1.01
0.05	1.05
0.10	1.11
0.20	1.25
0.30	1.43
0.40	1.67
0.50	2.00
0.60	2.50
0.70	3.33
0.80	5.00
0.90	10.00
1.00	∞

[a]Calculated from equation (4). Φ_x is the quantum yield for e- flow in the external circuit (photocurrent) and Φ_{r_o}/Φ_r is the ratio of the emission quantum yield between open circuit ($\Phi_x = 0$) and the potential where Φ_x was measured.

Figure Captions

Figure 1. (a) Comparison of penetration depths for band gap edge (514.5 nm) and ultraband gap (501.7 nm) excitation relative to the width of the depletion region at temperature T_1 for CdS:Te (not to scale). E_{CB} and E_{VB} refer to the conduction and valence band energies. Doping CdS with Te is believed to introduce discrete states at energy E_{Te}. E_{BG} is the band gap energy at T_1; (b) at temperature $T_2 > T_1$ the band gap is expected to shrink, $E'_{BG} < E_{BG}$; as a consequence, the penetration depth of 514.5 nm light would be reduced; (c) the expected effect on the CdS:Te absorption spectrum caused by an increase in temperature. Solid and dashed lines represent the spectra at T_1 and T_2, respectively (curves are crude approximations and not drawn to scale).

Figure 2. Components of the CdS:Te-based variable temperature PEC: (1) n-type CdS:Te photoelectrode, site of polyselenide oxidation; (2) thermometer; (3) Pt foil counterelectrode, site of polyselenide reduction; (4) Ag pseudoreference electrode (PRE); (5) rubber stopper, positioned loosely enough to serve as a vent, through which (1)-(4) are inserted; (6) magnetic stir bar; (7) aqueous polyselenide electrolyte; (8) nichrome wire wound outside the cell for resistive heating; (9) N_2 inlet, the N_2 passing first through an aqueous reservoir. Components (1), (3), and (4) are connected to a potentiostat.

Figure 3. Uncorrected emission spectra at open circuit of a CdS:Te electrode in 5M OH^-/0.09 M Se^{2-}/0.001 M Se_2^{2-} electrolyte. Temperature and excitation wavelength employed for each curve are identified in the figure. Although the curves have all been normalized to the same intensity at λ_{max} ~600 nm, the number above each curve gives the actual intensity before normalization. A filter solution was used to eliminate the exciting light (see Experimental) and is responsible for the deviations from baseline at the short wavelength extreme.

Figure 4. (a) Relative emission intensity monitored at 600 nm vs. temperature in polyselenide electrolyte (5M OH^-/0.09M Se^{2-}/0.001M Se_2^{2-}) of CdS:Te excited at open circuit with 501.7 nm (circles) and 514.5 nm (squares) light. The excitation intensity at 501.7 nm is 6X that at 514.5 nm in order to approximately match emission intensity at room temperature; (b) relative emission intensity vs. temperature for 514.5 nm excitation of a CdS:Te electrode (different sample than in (a)) in polyselenide electrolyte (5M OH^-/0.02M Se^{2-}/0.001M Se_2^{2-}) at three potentials. Circles, squares and triangles correspond to open circuit, 0.0 V, and 0.7 V vs. Ag(PRE), respectively; (c) relative emission intensity vs. temperature for the same electrode and geometric configuration as in (b), but now excited with an equivalent number of 501.7 nm photons as in (b). The point "100" on the emission scale is ~one-fifth the corresponding point in (b). The symbols in (c) have the same significance in terms of potential as in (b). Typical photocurrent behavior at 0.7 V accompanying the emission changes shown in (b) and (c) is given in Figure 5a.

Figure 5. (a) Relative photocurrent vs. temperature for a CdS:Te electrode in aqueous polyselenide electrolyte (5M OH^-/0.02M Se^{2-}/0.001M Se_2^{2-}) excited with equivalent photons of 514.5 nm (filled circles) or 501.7 nm (open circles) light at 0.7 V vs Ag(PRE). The scale is such that the photocurrent at 25°C from 501.7 nm excitation has been arbitrarily set at 100 and corresponds to a current density of ~0.36 mA/cm^2 and a quantum yield for electron flow, Φ_x, of ~0.50; (b) relative photocurrent vs. temperature for an undoped CdS electrode in the same electrolyte as in (a), excited with an equivalent photon flux of 514.5 nm (filled circles) and 501.7 nm (open circles) light. Again, "100" has been arbitrarily set as the 25°C photocurrent from 501.7 nm excitation and represents a current density of ~0.44 mA/cm^2 and a Φ_x of ~0.60.

Figure 6. Current-luminescence-voltage curves (iLV) for a CdS:Te electrode in polyselenide electrolyte. Unprimed, solid line curves are photocurrent (left hand scale) and primed, dotted line curves are luminescence intensity (right hand scale) monitored at λ_{max}, ~600 nm. A and A' were obtained from excitation at 501.7 nm, 23°C; B and B' from 514.5 nm, 23°C; C and C' from 501.7 nm, 49°C; D and D' from 514.5 nm and 86°C. Note that the ordinate of D' has been expanded by a factor of 10. Equivalent numbers of 501.7 and 514.5 nm photons were used in identical PEC geometric configurations. The exposed electrode area is ~0.41 cm^2 and the estimated value of Φ_x for 501.7 nm excitation at 23°C and 0.7 V vs. Ag(PRE) is ~ 0.50, uncorrected for reflection losses and solution absorbance.

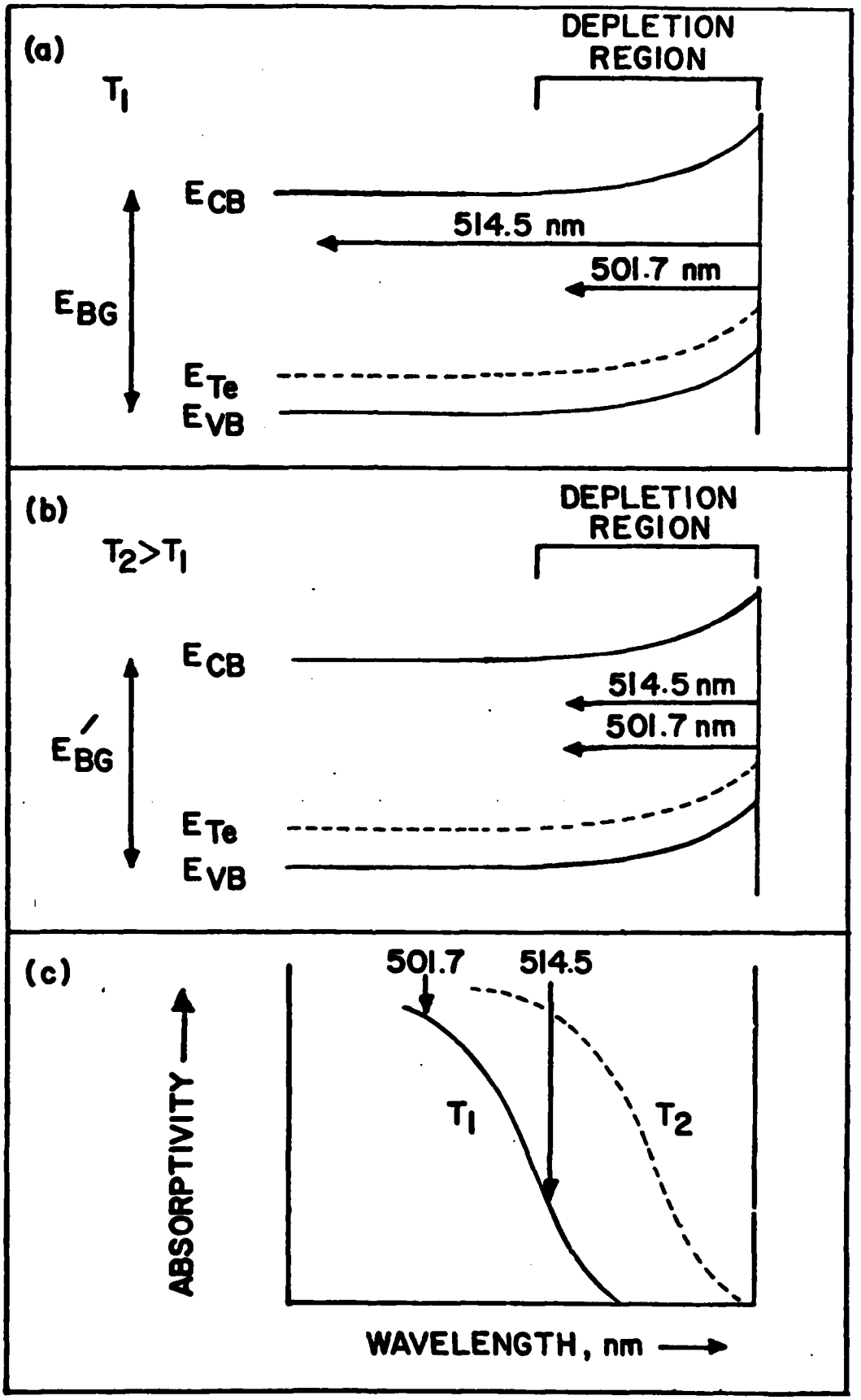
(a)
DEPLETION REGION
T_1
E_{CB}
514.5 nm
501.7 nm
E_{BG}
E_{Te}
E_{VB}
(b)
DEPLETION REGION
$T_2 > T_1$
E_{CB}
514.5 nm
501.7 nm
E'_{BG}
E_{Te}
E_{VB}
(c)
501.7
514.5
T_1
T_2
ABSORPTIVITY
WAVELENGTH, nm

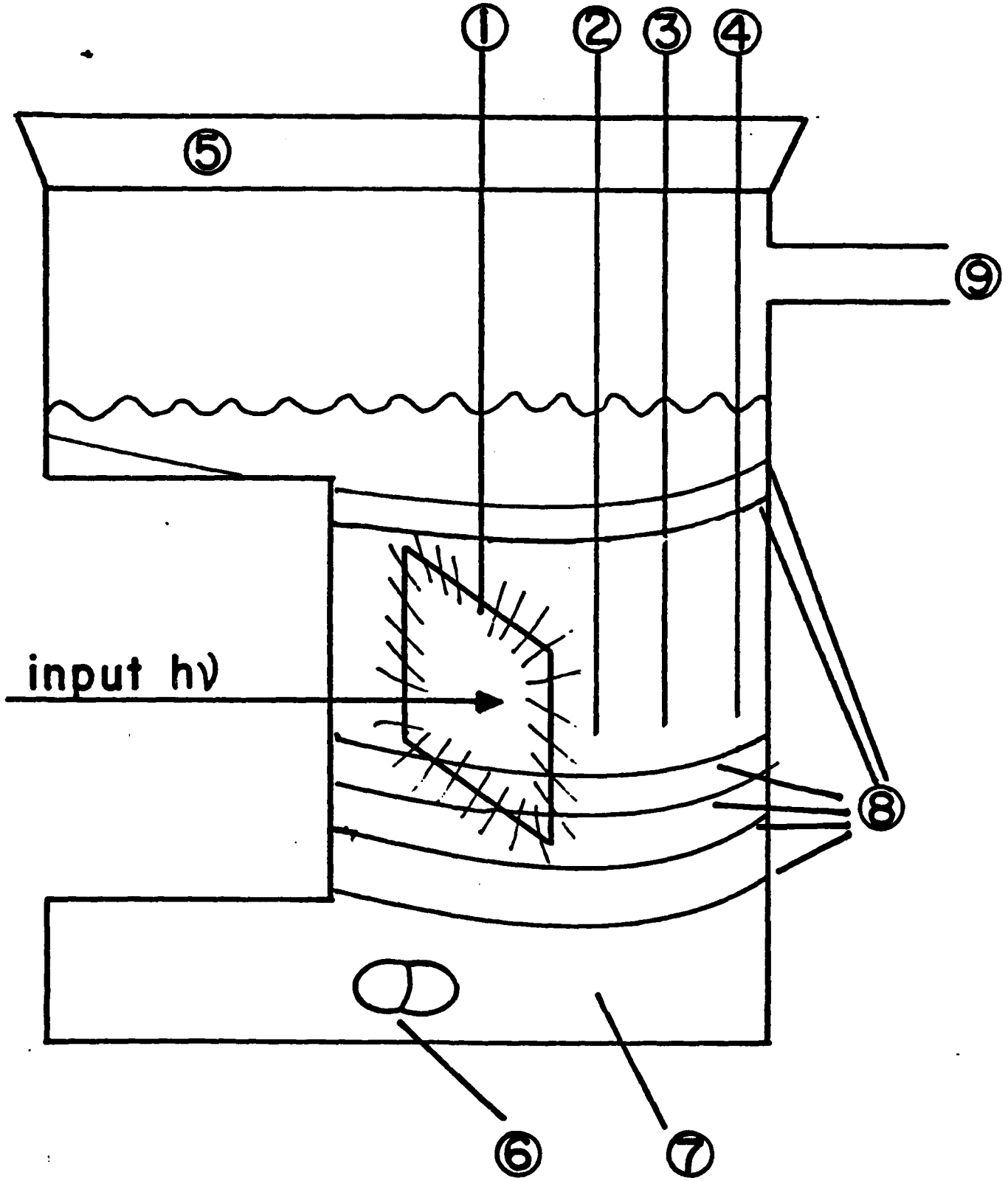
①
②
③
④
⑤
⑨
input hν
⑧
⑥
⑦

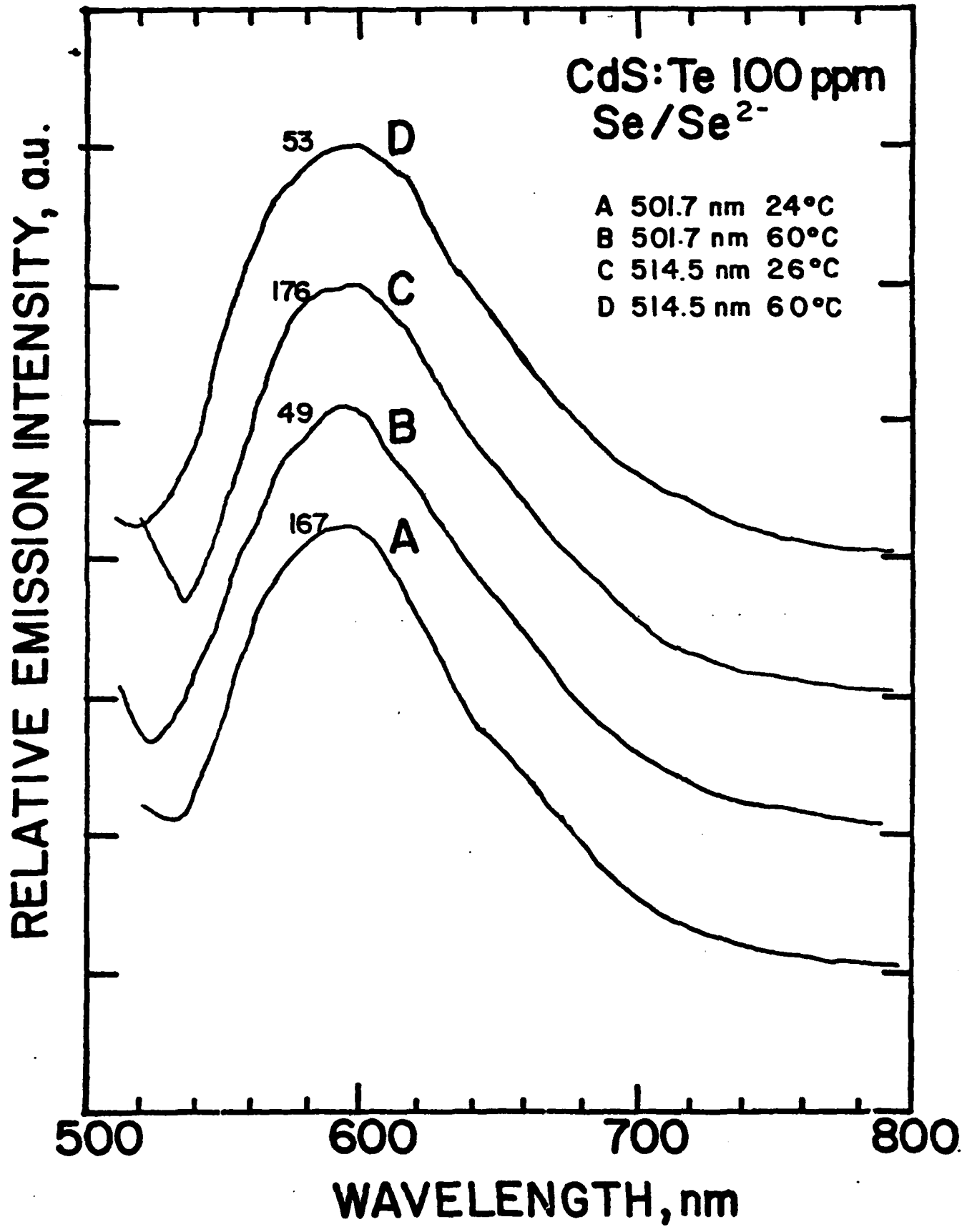
CdS:Te 100 ppm
Se/Se2-
A 501.7 nm 24°C
B 501.7 nm 60°C
C 514.5 nm 26°C
D 514.5 nm 60°C
53
D
176
C
49
B
167
A
RELATIVE EMISSION INTENSITY, a.u.
500
600
700
800
WAVELENGTH, nm

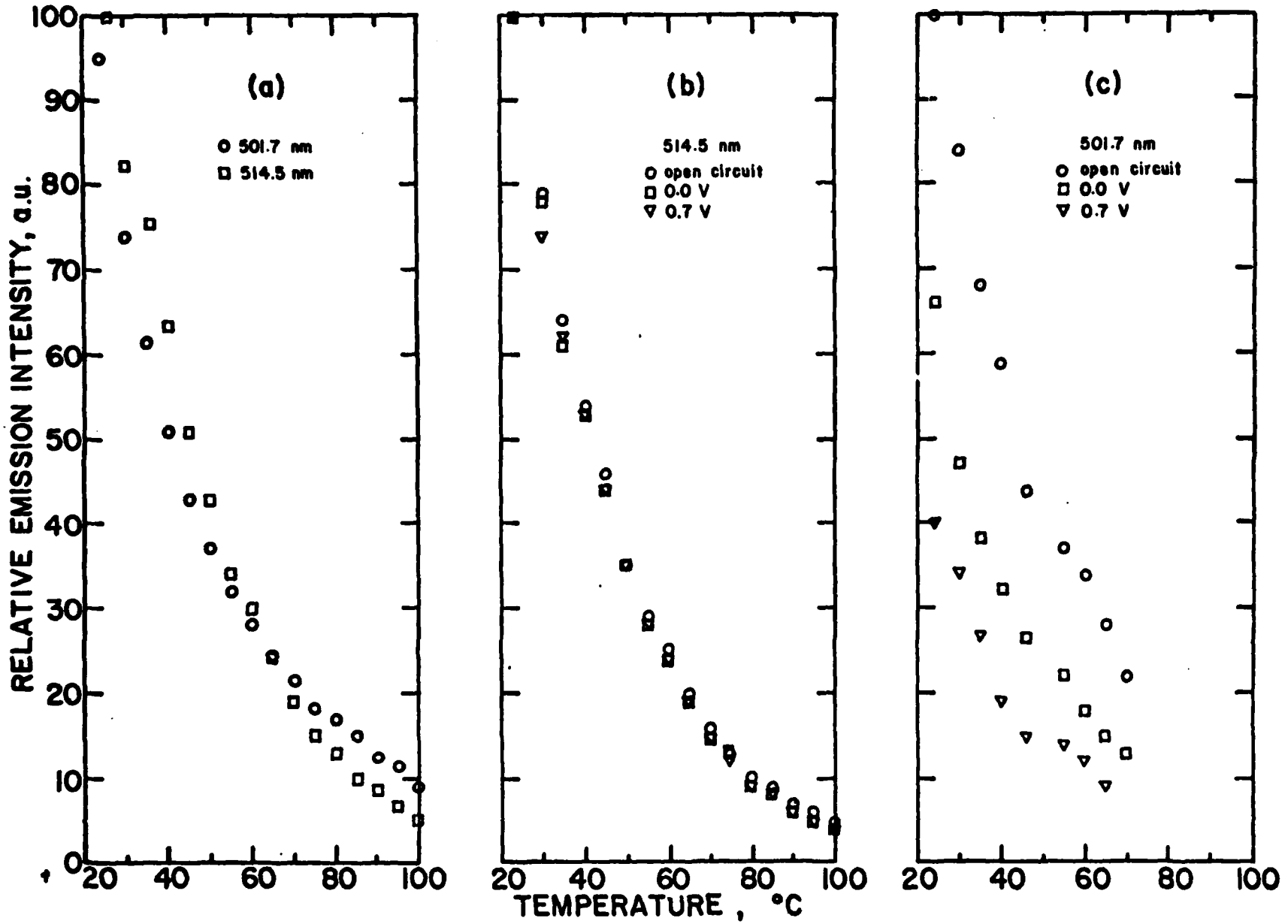
(a)
○ 501.7 nm
□ 514.5 nm
(b)
514.5 nm
○ open circuit
□ 0.0 V
▽ 0.7 V
(c)
501.7 nm
○ open circuit
□ 0.0 V
▽ 0.7 V
RELATIVE EMISSION INTENSITY, a.u.
TEMPERATURE , °C
0
10
20
30
40
50
60
70
80
90
100
20
40
60
80
100

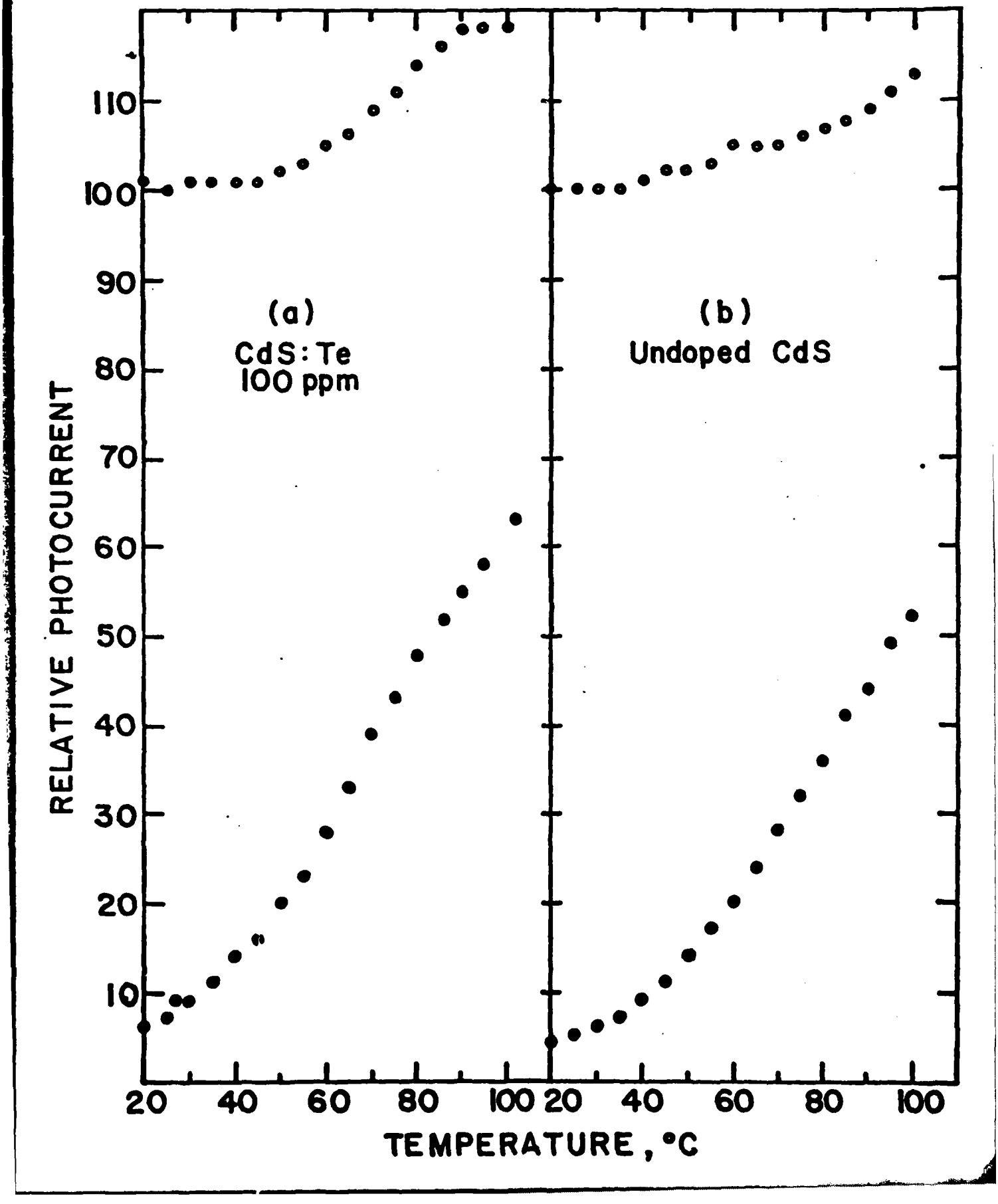
RELATIVE PHOTOCURRENT
110
100
90
80
70
60
50
40
30
20
10
(a)
CdS:Te
100 ppm
(b)
Undoped CdS
20
40
60
80
100
20
40
60
80
100
TEMPERATURE, °C

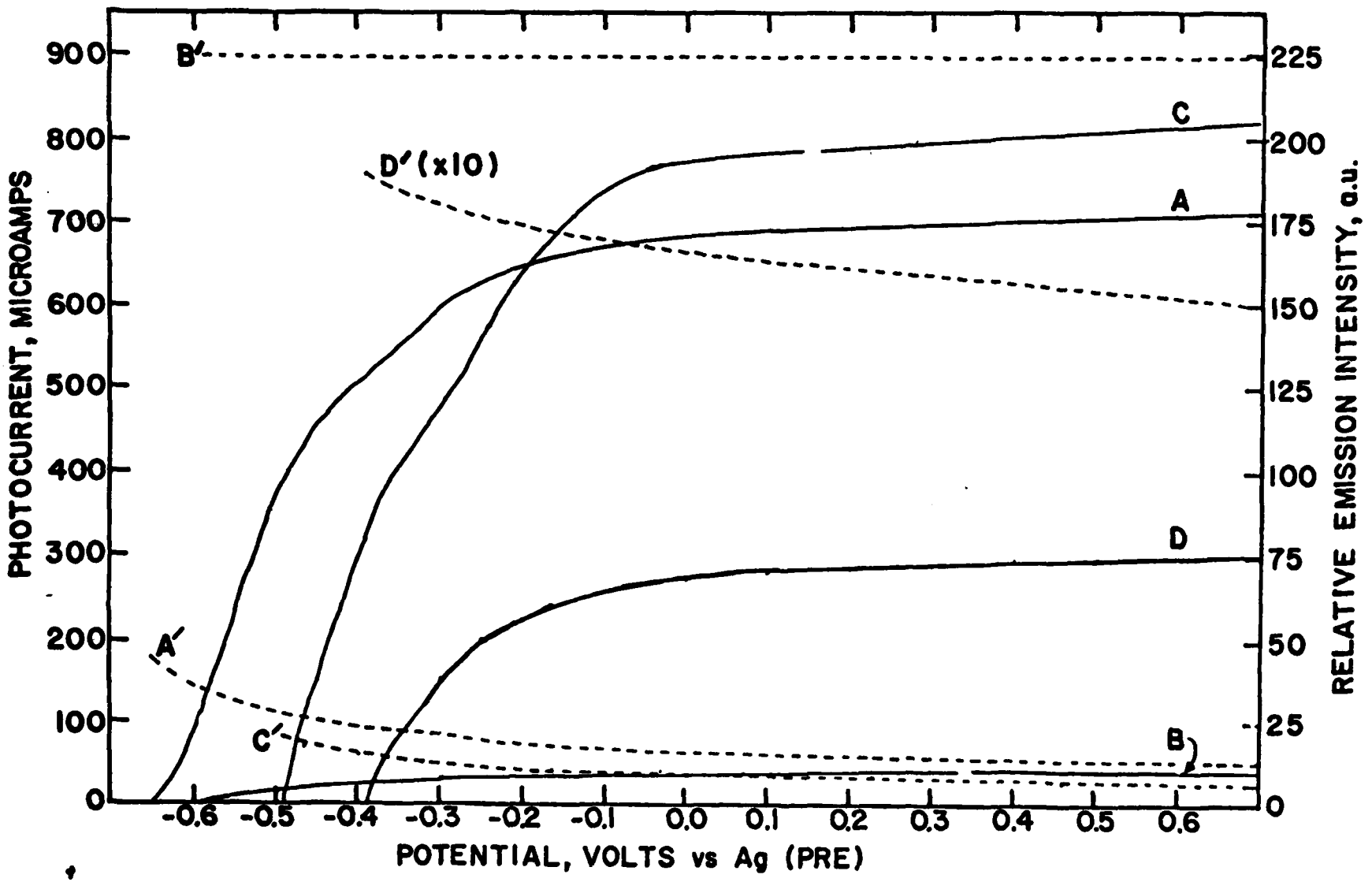
PHOTOCURRENT, MICROAMPS
RELATIVE EMISSION INTENSITY, a.u.
POTENTIAL, VOLTS vs Ag (PRE)
900
800
700
600
500
400
300
200
100
0
225
200
175
150
125
100
75
50
25
0
-0.6
-0.5
-0.4
-0.3
-0.2
-0.1
0.0
0.1
0.2
0.3
0.4
0.5
0.6
B'
D'(x10)
C
A
D
A'
C'
B

TECHNICAL REPORT DISTRIBUTION LIST, GEN

	No. Copies
Office of Naval Research Attn: Code 472 800 North Quincy Street Arlington, Virginia 22217	2
ONR Branch Office Attn: Dr. George Sandoz 536 S. Clark Street Chicago, Illinois 60605	1
ONR Area Office Attn: Scientific Dept. 715 Broadway New York, New York 10003	1
ONR Western Regional Office 1030 East Green Street Pasadena, California 91106	1
ONR Eastern/Central Regional Office Attn: Dr. L. H. Peebles Building 114, Section D 666 Summer Street Boston, Massachusetts 02210	1
Director, Naval Research Laboratory Attn: Code 6100 Washington, D.C. 20390	1
The Assistant Secretary of the Navy (RE&S) Department of the Navy Room 4E736, Pentagon Washington, D.C. 20350	1
Commander, Naval Air Systems Command Attn: Code 310C (H. Rosenwasser) Department of the Navy Washington, D.C. 20360	1
Defense Technical Information Center Building 5, Cameron Station Alexandria, Virginia 22314	12
Dr. Fred Saalfeld Chemistry Division, Code 6100 Naval Research Laboratory Washington, D.C. 20375	1
U.S. Army Research Office Attn: CRD-AA-IP P.O. Box 1211 Research Triangle Park, N.C. 27709	1
Naval Ocean Systems Center Attn: Mr. Joe McCartney San Diego, California 92152	1
Naval Weapons Center Attn: Dr. A. B. Amster, Chemistry Division China Lake, California 93555	1
Naval Civil Engineering Laboratory Attn: Dr. R. W. Drisko Port Hueneme, California 93401	1
Department of Physics & Chemistry Naval Postgraduate School Monterey, California 93940	1
Dr. A. L. Slafkosky Scientific Advisor Commandant of the Marine Corps (Code RD-1) Washington, D.C. 20380	1
Office of Naval Research Attn: Dr. Richard S. Miller 800 N. Quincy Street Arlington, Virginia 22217	1
Naval Ship Research and Development Center Attn: Dr. G. Bosmajian, Applied Chemistry Division Annapolis, Maryland 21401	1
Naval Ocean Systems Center Attn: Dr. S. Yamamoto, Marine Sciences Division San Diego, California 91232	1
Mr. John Boyle Materials Branch Naval Ship Engineering Center Philadelphia, Pennsylvania 19112	1

TECHNICAL REPORT DISTRIBUTION LIST, GEN

	No. Copies
Dr. Rudolph J. Marcus Office of Naval Research Scientific Liaison Group American Embassy APO San Francisco 96503	1
Mr. James Kelley DTNSRDC Code 2803 Annapolis, Maryland 21402	1

TECHNICAL REPORT DISTRIBUTION LIST, 359

	No. Copies
Dr. Paul Delahay Department of Chemistry New York University New York, New York 10003	1
Dr. E. Yeager Department of Chemistry Case Western Reserve University Cleveland, Ohio 41106	1
Dr. D. N. Bennion Department of Chemical Engineering Brigham Young University Provo, Utah 84602	1
Dr. R. A. Marcus Department of Chemistry California Institute of Technology Pasadena, California 91125	1
Dr. J. J. Auborn Bell Laboratories Murray Hill, New Jersey 07974	1
Dr. Adam Heller Bell Laboratories Murray Hill, New Jersey 07974	1
Dr. T. Katan Lockheed Missiles & Space Co, Inc. P.O. Box 504 Sunnyvale, California 94088	1
Dr. Joseph Singer, Code 302-1 NASA-Lewis 21000 Brookpark Road Cleveland, Ohio 44135	1
Dr. B. Brummer EIC Incorporated 55 Chapel Street Newton, Massachusetts 02158	1
Library P. R. Mallory and Company, Inc. Northwest Industrial Park Burlington, Massachusetts 01803	1
Dr. P. J. Hendra Department of Chemistry University of Southhampton Southhampton SO9 5NH United Kingdom	1
Dr. Sam Perone Department of Chemistry Purdue University West Lafayette, Indiana 47907	1
Dr. Royce W. Murray Department of Chemistry University of North Carolina Chapel Hill, North Carolina 27514	1
Naval Ocean Systems Center Attn: Technical Library San Diego, California 92152	1
Dr. C. E. Mueller The Electrochemistry Branch Materials Division, Research & Technology Department Naval Surface Weapons Center White Oak Laboratory Silver Spring, Maryland 20910	1
Dr. G. Goodman Globe-Union Incorporated 5757 North Green Bay Avenue Milwaukee, Wisconsin 53201	1
Dr. J. Boechler Electrochimica Corporation Attention: Technical Library 2485 Charleston Road Mountain View, California 94040	1
Dr. P. P. Schmidt Department of Chemistry Oakland University Rochester, Michigan 48063	1
Dr. H. Richtol Chemistry Department Rensselaer Polytechnic Institute Troy, New York 12181	1

TECHNICAL REPORT DISTRIBUTION LIST, 359

	No. Copies
Dr. A. B. Ellis Chemistry Department University of Wisconsin Madison, Wisconsin 53706	1
Dr. M. Wrighton Chemistry Department Massachusetts Institute of Technology Cambridge, Massachusetts 02139	1
Larry E. Plew Naval Weapons Support Center Code 30736, Building 2906 Crane, Indiana 47522	1
S. Ruby DOE (STOR) 600 E Street Washington, D.C. 20545	1
Dr. Aaron Wold Brown University Department of Chemistry Providence, Rhode Island 02192	1
Dr. R. C. Chudacek McGraw-Edison Company Edison Battery Division Post Office Box 28 Bloomfield, New Jersey 07003	1
Dr. A. J. Bard University of Texas Department of Chemistry Austin, Texas 78712	1
Dr. M. M. Nicholson Electronics Research Center Rockwell International 3370 Miraloma Avenue Anaheim, California	1
Dr. Donald W. Ernst Naval Surface Weapons Center Code R-33 White Oak Laboratory Silver Spring, Maryland 20910	1
Dr. R. P. Van Duyne Department of Chemistry Northwestern University Evanston, Illinois 60201	1
Dr. B. Stanley Pons Department of Chemistry University of Alberta Edmonton, Alberta CANADA T6G 2G2	1
Dr. Michael J. Weaver Department of Chemistry Michigan State University East Lansing, Michigan 48824	1
Dr. R. David Rauh EIC Corporation 55 Chapel Street Newton, Massachusetts 02158	1
Dr. J. David Margerum Research Laboratories Division Hughes Aircraft Company 3011 Malibu Canyon Road Malibu, California 90265	1
Dr. Martin Fleischmann Department of Chemistry University of Southampton Southampton 509 5NH England	1
Dr. Janet Osteryoung Department of Chemistry State University of New York at Buffalo Buffalo, New York 14214	1
Dr. R. A. Osteryoung Department of Chemistry State University of New York at Buffalo Buffalo, New York 14214	1
Mr. James R. Moden Naval Underwater Systems Center Code 3632 Newport, Rhode Island 02840	1

TECHNICAL REPORT DISTRIBUTION LIST, 359

	No. Copies
Dr. R. Nowak Naval Research Laboratory Code 6130 Washington, D.C. 20375	1
Dr. John F. Houlihan Shenango Valley Campus Pennsylvania State University Sharon, Pennsylvania 16146	1
Dr. M. G. Sceats Department of Chemistry University of Rochester Rochester, New York 14627	1
Dr. D. F. Shriver Department of Chemistry Northwestern University Evanston, Illinois 60201	1
Dr. D. H. Whitmore Department of Materials Science Northwestern University Evanston, Illinois 60201	1
Dr. Alan Bewick Department of Chemistry The University Southampton, S09 5NH England	1
Dr. A. Himy NAVSEA-5433 NC #4 2541 Jefferson Davis Highway Arlington, Virginia 20362	1
Dr. John Kincaid Department of the Navy Stategic Systems Project Office Room 901 Washington, DC 20376	1
M. L. Robertson Manager, Electrochemical Power Sonices Division Naval Weapons Support Center Crane, Indiana 47522	1
Dr. Elton Cairns Energy & Environment Division Lawrence Berkeley Laboratory University of California Berkeley, California 94720	1
Dr. Bernard Spielvogel U.S. Army Research Office P.O. Box 12211 Research Triangle Park, NC 27709	1
Dr. Denton Elliott Air Force Office of Scientific Research Bldg. 104 Bolling AFB Washington, DC 20332	1

TECHNICAL REPORT DISTRIBUTION LIST, 051C

	No. Copies
Dr. M. B. Denton Department of Chemistry University of Arizona Tucson, Arizona 85721	1
Dr. R. A. Osteryoung Department of Chemistry State University of New York at Buffalo Buffalo, New York 14214	1
Dr. B. R. Kowalski Department of Chemistry University of Washington Seattle, Washington 98105	1
Dr. S. P. Perone Department of Chemistry Purdue University Lafayette, Indiana 47907	1
Dr. D. L. Venezky Naval Research Laboratory Code 6130 Washington, D.C. 20375	1
Dr. H. Freiser Department of Chemistry University of Arizona Tuscon, Arizona 85721	
Dr. Fred Saalfeld Naval Research Laboratory Code 6110 Washington, D.C. 20375	1
Dr. H. Chernoff Department of Mathematics Massachusetts Institute of Technology Cambridge, Massachusetts 02139	1
Dr. K. Wilson Department of Chemistry University of California, San Diego La Jolla, California	1
Dr. A. Zirino Naval Undersea Center San Diego, California 92132	1
Dr. John Duffin United States Naval Postgraduate School Monterey, California 93940	1
Dr. G. M. Hieftje Department of Chemistry Indiana University Bloomington, Indiana 47401	1
Dr. Victor L. Rehn Naval Weapons Center Code 3813 China Lake, California 93555	1
Dr. Christie G. Enke Michigan State University Department of Chemistry East Lansing, Michigan 48824	1
Dr. Kent Eisentraut, MBT Air Force Materials Laboratory Wright-Patterson AFB, Ohio 45433	1
Walter G. Cox, Code 3632 Naval Underwater Systems Center Building 148 Newport, Rhode Island 02840	1
Professor Isiah M. Warner Texas A&M University Department of Chemistry College Station, Texas 77840	1
Professor George H. Morrison Cornell University Department of Chemisty Ithaca, New York 14853	1